

STRUCTURE OF INORGANIC COMPOUNDS

Crystal Structure of Niobium-Rich Lomonosovite with Symmetry *P1* from the Khibiny Massif (Kola Peninsula)

R. K. Rastsvetaeva^{a,*}, V. A. Zaitsev^b, and I. V. Pekov^{b,c}

^a *Shubnikov Institute of Crystallography, Federal Scientific Research Centre “Crystallography and Photonics,”
Russian Academy of Sciences, Moscow, 119333 Russia*

^b *Vernadsky Institute of Geochemistry and Analytical Chemistry, Russian Academy of Sciences, Moscow, 119334 Russia*

^c *Moscow State University, Moscow, Russia*

*e-mail: rast@crys.ras.ru

Received October 19, 2019; revised November 8, 2019; accepted November 14, 2019

Abstract—A new niobium-rich lomonosovite variety with a high degree of ordering of Ti and Nb atoms has been investigated by X-ray diffraction analysis and electron probe microanalysis. Its simplified formula is $\text{Na}_{10}\text{Ti}_2(\text{Nb,Fe,Ti})_2(\text{Si}_2\text{O}_7)_2(\text{PO}_4)_2\text{O}_4$. The triclinic unit-cell parameters are $a = 5.411(1) \text{ \AA}$, $b = 7.108(1) \text{ \AA}$, $c = 14.477(2) \text{ \AA}$, $\alpha = 99.78(1)^\circ$, $\beta = 96.59(1)^\circ$, $\gamma = 90.26(1)^\circ$, $V = 544.94(5) \text{ \AA}^3$, $Z = 1$, sp. gr. *P1*. The crystal structure has been refined to the final reliability factor $R = 6.3\%$ within the anisotropic approximation of atomic displacements using 3674 reflections with $F > 3\sigma(F)$. The problem of niobium distribution in minerals with structures of lomonosovite and related types is discussed.

DOI: 10.1134/S1063774520030268

INTRODUCTION

Lomonosovite (phosphate–silicate with the idealized formula $\text{Na}_{10}\text{Ti}_4(\text{Si}_2\text{O}_7)_2(\text{PO}_4)_2\text{O}_4$) was described by V.I. Gerasimovskii [1] as a new mineral species in peralkaline pegmatites of the Lovozero alkaline massif on the Kola Peninsula. The first structural model for lomonosovite was proposed in 1965 [2]; however, the structure was completely determined only in 1971 [3] from the scans of layer lines in rotation X-ray diffraction patterns within the triclinic unit cell with the following parameters: $a = 5.44 \text{ \AA}$, $b = 7.163 \text{ \AA}$, $c = 14.83 \text{ \AA}$, $\alpha = 99^\circ$, $\beta = 106^\circ$, and $\gamma = 90^\circ$. This structure was repeatedly solved within the cell with $A = 5.49 \text{ \AA}$, $B = 7.11 \text{ \AA}$, $C = 14.50 \text{ \AA}$, $\alpha = 101^\circ$, $\beta = 96^\circ$, and $\gamma = 90^\circ$ [4], which is related to the previous one via the transition matrix: $A = -a$, $B = b$, $C = a + c$ (the coordinates are, respectively, $X = -x + z$, $Y = y$, $Z = z$). Both models are identical; they were refined in the centrosymmetric version (sp. gr. $P\bar{1}$) with isomorphic impurities disregarded. The distribution of impurity cations at the key *M* sites was also established on a sample from the Lovozero alkaline massif [5]. The structural model was refined in the centrosymmetric version with the following unit-cell parameters: $a = 5.4170(7) \text{ \AA}$, $b = 7.1190(9) \text{ \AA}$, $c = 14.487(2) \text{ \AA}$, $\alpha = 99.957(3)^\circ$, $\beta = 96.711(3)^\circ$, and $\gamma = 90.360(3)^\circ$.

The crystal structure of lomonosovite (as well as the other heterophyllosilicates) is based on three-layer *HOH* packets consisting of a central octahedral *O* layer

and two outer heteropolyhedral *H* layers. Ti- and Na-centered octahedra are distinguished in the *O* layer, whereas the *H* layers are composed of Ti-centered octahedra and Si_2O_7 diorthogroups. The interpacket space includes Na^+ cations and PO_4^{3-} anions [3, 4].

In this study, we investigate a lomonosovite sample from the Umbitovoe ultraagpaite pegmatite body opened in the Koashva quarry, aimed at mining the apatite deposit of the same name at the Koashva mountain in the south-east part of the Khibiny alkaline massif neighboring the Lovozero massif. Lomonosovite was found in the form of dark-brown lamellar crystals up to $1 \times 1.5 \times 3 \text{ cm}$ in size in association with entangled fiber aegirine, colorless pectolite, and gray-green microcline. The internal structure of the lomonosovite crystal is inhomogeneous. It consists of irregularly intermittent portions of a contrast chemical composition of two types: “normal” lomonosovite containing 2.7–4.0 wt % Nb_2O_5 and niobium-rich variety with the maximally high (among the lomonosovite samples that have been studied to date) niobium content (10.1–11.8 wt % Nb_2O_5); this sample is also characterized by higher Mn, Fe, and Ca contents (Table 1). It also differs from “normal” lomonosovite by the symmetry and structural features. These two samples have no optical differences but are distinguished in a scanning electron microscope in the backscattered-electron mode due to the significant enrichment of one of the samples in heavy Nb cations. The interfaces between portions of these lomonosovite

Table 1. Chemical composition of lomonosovite (wt %)

Component	“Niobium” lomonosovite		“Normal” lomonosovite [6]		Limits of variation for lomonosovite on the whole [6]
	average content	limits	average content	limits	
Na ₂ O	27.25	26.88–27.69	29.00	28.17–29.62	24.00–30.24
MgO	0.48	0.37–0.58	0.24	0.10–0.36	0–0.87
Al ₂ O ₃	0.00	0.00–0.02	0.02	0.00–0.08	0.00–0.54
SiO ₂	23.53	23.23–23.85	22.43	23.95–24.26	21.99–24.80
P ₂ O ₅	13.48	13.38–13.61	14.06	13.88–14.18	12.23–14.62
CaO	1.78	1.48–1.98	1.08	0.81–1.40	0.28–3.03
TiO ₂	19.12	18.18–19.80	26.88	24.64–28.14	15.00–26.51
MnO	1.92	1.80–2.07	0.71	0.48–0.92	0.00–4.56
FeO	2.43	2.11–2.60	1.15	0.57–1.46	0.52–2.81
Nb ₂ O ₅	10.71	10.08–11.77	3.34	2.69–3.98	0.00–10.66
F	0.42	0.32–0.51	0.19	0.11–0.37	
–O=F ₂	–0.18		–0.08		
In total	100.50		98.91		

variety are sharp. The sizes of chemically uniform portions are as large as 0.3×0.3 mm, which made it possible, in particular, to select a single-crystal sample of niobium-rich lomonosovite applicable for X-ray diffraction analysis.

Table 2. Crystallographic characteristics, details of the X-ray experiment, and parameters of the structure refinement

Idealized formula ($Z = 1$)	Na ₁₀ Ti ₂ (Nb, Fe, Ti) ₂ (Si ₂ O ₇) ₂ (PO ₄) ₂ O ₄
$a, b, c, \text{Å}$	5.411(1), 7.108(1), 14.477(2)
$\alpha, \beta, \gamma, \text{deg}$	99.78(1), 96.59(1), 90.26(1)
$V, \text{Å}^3$	544.94(5)
System, sp. gr., Z	triclinic, $P1, 1$
Crystal sizes, mm	$0.2 \times 0.15 \times 0.1$
Diffraction	Xcalibur Eos CCD Oxford Diffraction
Radiation; $\lambda, \text{Å}$	MoK α ; 0.71073
Scan mode	ω
Ranges of indices h, k, l	$-12 < h < 12, -14 < k < 16,$ $-15 < l < 15$
$(\sin\theta/\lambda)_{\max}$	0.798
Numbers of reflections: measured/unique with $F > 3\sigma F$	19061/3674
R_{av}	0.056
Refinement method	least-squares based on F
$R, \%$	0.063
Program	AREN [7]

EXPERIMENTAL

The chemical composition of the mineral was investigated by electron probe microanalysis on a Camebax Microbeam device at an accelerating voltage of 15 kV and a beam current of 30 nA (Vernadsky Institute of Geochemistry and Analytical Chemistry of the Russian Academy of Sciences, analyst V.G. Senin). The analysis results are listed in Table 1. The empirical formula was calculated for the sum $(\text{Si} + \text{P}) = 6$ to be Na_{9.06}Mg_{0.12}Si_{4.04}P_{1.96}Ca_{0.33}Ti_{2.46}Mn_{0.28}Fe_{0.35}Nb_{0.83}F_{0.23}O_{25.47}.

The diffraction data were collected from a single-crystal fragment in the form of a thin plate. The triclinic unit-cell parameters are $a = 5.411(1) \text{ Å}$, $b = 7.108(1) \text{ Å}$, $c = 14.477(2) \text{ Å}$, $\alpha = 99.78(1)^\circ$, $\beta = 96.59(1)^\circ$, and $\gamma = 90.26(1)^\circ$. The crystallographic characteristics and details of the X-ray experiment are given in Table 2.

Although the heteropolyhedral three-layer packet in the structure of the lomonosovite under study is topologically centrosymmetric, the statistical analysis of the distribution of structural Wilson factors suggested that the structure may be acentric. The structure model was found by direct methods using the “phase correction” procedure in the AREN software [7] within the sp. gr. $P1$. The structural parameters were refined within the anisotropic approximation. Mixed atomic scattering curves were applied for octahedrally coordinated cation sites. All the calculations were performed using the AREN crystallographic package [7]. The refined structural parameters and characteristics of coordination polyhedra are listed in Tables 3 and 4, respectively.

DESCRIPTION OF THE STRUCTURE
AND DISCUSSION OF THE RESULTS

The main specific features of the composition and structure of the niobium-rich lomonosovite variety under study are indicated by its crystallochemical formula ($Z=1$), which is in good agreement with the empirical formula obtained by the electron-probe analysis: $\text{Na}_7(\text{Na}_{0.67}\text{Ca}_{0.33})[\text{Na}_2(\text{Nb}_{0.48}\text{Mn}_{0.28}\text{Ti}_{0.24})(\text{Ti}_{0.82}\text{Mg}_{0.18})]$

$[(\text{Ti}_{0.65}\text{Nb}_{0.35})(\text{Ti}_{0.65}\text{Fe}_{0.35}^{2+})][\text{Si}_2\text{O}_7]_2[\text{PO}_4]_2\text{O}_{3.53}\text{F}_{0.47}$. The simplified formula is $\text{Na}_{10}\text{Ti}_2(\text{Nb},\text{Fe},\text{Ti})_2(\text{Si}_2\text{O}_7)_2(\text{PO}_4)_2\text{O}_4$.

The iron cation charge is assumed to be divalent because the cation–anion distance in the *M4* octahedron is consistent with the ionic radius of 0.56–0.57 Å (an intermediate value between the ionic radii for Fe^{2+} (0.61 Å) and Fe^{3+} (0.55 Å)) and corresponds to the mixed-valence iron state. Taking into account that the iron content in the *M4* site is only one third of the total, it is unreliable to use these distances to find the dominant valence.

The heteropolyhedral three-layer structural modulus of this acentric (sp. gr. *P1*) lomonosovite variety (as well as in the other heterophyllosilicates [8]) consists of the central *O* layer of close-packed octahedra with shared edges and *H* layers (adjacent to the central layer from two sides), formed by diorthogroups $[\text{Si}_2\text{O}_7]$ and discrete octahedra (Figs. 1, 2). The *M1* and *M2* octahedra of the *O* layer with identical mean *M*–*O* distances of 2.043 Å are statistically and differently occupied by cations: Nb atoms enter only the *M1* octahedron, where they dominate over all other cations (0.48Nb + 0.28Mn + 0.24Ti). The peripheral *M3* and *M4* octahedra (with the *M*–*O* distances of 1.96 and 1.97 Å, respectively) also exhibit mixed site occupancy, and Nb atoms also enter only one of them (Table 4).

Na-centered octahedra Na1 and Na2 of the *O* layer are characterized by mean cation–anion distances of 2.47 and 2.44 Å. Single PO_4 tetrahedra share an oxygen vertex with the *M3* and *M4* octahedra, involved in the aggregation of the packets into a three-dimensional structure, along with interpacket atoms Na3–Na10, whose coordination numbers change from four to eight, whereas the mean cation–anion distances vary within 2.30–2.57 Å. Impurity Ca atoms enter the Na3 eight-vertex polyhedron with a mean Na3–*O* distance of 2.52 Å (Table 4). The found distribution of cations revealed the main reason for the absence of center of symmetry: incorporation of a large amount of niobium in only one of two (*M1*–*M2* and *M3*–*M4*) octahedra linked by a pseudocenter of symmetry.

Lomonosovite belongs to heterophyllosilicates [8, 9] and has unit-cell sizes, chemical composition, and symmetry and topological characteristics close to those of β -lomonosovite (primarily) and vuonnemite, whose simplified formulas are, respectively, $\text{Na}_{5+x}\text{Ti}_4[\text{Si}_2\text{O}_7]_2[\text{PO}_3(\text{OH})]_{2-y}[\text{PO}_2(\text{OH})_2]_y\text{O}_2[(\text{OH},\text{F})_{2-z}\text{O}_z]$ (where $0 \leq x \leq 2$, $0 \leq y \leq 1$, and $0 \leq z \leq 1$) and

Table 3. Site coordinates and equivalent atomic displacement parameters

Site	<i>x/a</i>	<i>y/b</i>	<i>z/c</i>	$B_{\text{eq}}, \text{Å}^2$
<i>M1</i>	0.7573(1)	0.2102(1)	0.8513(1)	1.17(2)
<i>M2</i>	0.3039(4)	0.9860(3)	0.8362(1)	0.70(3)
<i>M3</i>	0.6896(2)	0.5267(1)	0.0613(1)	0.74(2)
<i>M4</i>	0.3599(2)	0.6716(2)	0.6267(1)	0.64(3)
Si1	0.8773(5)	0.9610(3)	0.6462(2)	0.33(7)
Si2	0.8630(4)	0.3960(3)	0.6663(2)	0.35(7)
Si3	0.1760(5)	0.2412(4)	0.0426(2)	0.85(7)
Si4	0.1913(5)	0.8032(4)	0.0208(2)	0.73(7)
P1	0.3471(4)	0.3753(3)	0.4103(2)	0.18(7)
P2	0.7031(5)	0.8249(4)	0.2758(2)	0.66(7)
Na1	0.7659(11)	0.7146(9)	0.8500(5)	1.9(1)
Na2	0.2805(9)	0.4811(7)	0.8415(5)	1.7(2)
Na3	0.2077(7)	0.5735(5)	0.2033(3)	1.53(5)
Na4	0.8434(10)	0.6244(7)	0.4821(4)	1.2(2)
Na5	0.6956(10)	0.0142(8)	0.0755(4)	1.2(2)
Na6	0.2861(12)	0.8591(8)	0.4302(4)	1.6(2)
Na7	0.7619(13)	0.3355(9)	0.2583(5)	1.8(2)
Na8	0.8454(11)	0.1360(8)	0.4449(4)	1.5(2)
Na9	0.3521(9)	0.1831(8)	0.6080(4)	1.5(2)
Na10	0.1995(12)	0.0548(8)	0.2407(5)	2.0(2)
O1*	0.1029(11)	0.8604(10)	0.5925(5)	0.5(3)
O2	0.7564(13)	0.6354(8)	0.2123(6)	0.8(3)
O3	0.9299(17)	0.9932(12)	0.7604(6)	1.1(3)
O4	0.9349(16)	0.3331(14)	0.0899(8)	1.5(2)
O5	0.1718(11)	0.7974(10)	0.9093(5)	0.4(2)
O6	0.8579(16)	0.1734(10)	0.6122(6)	0.8(3)
O7	0.6140(11)	0.8488(11)	0.5946(6)	0.7(2)
O8	0.2725(18)	0.2013(11)	0.4549(7)	1.4(2)
O9	0.0957(16)	0.4906(13)	0.6304(7)	1.3(2)
O10	0.6283(15)	0.3766(13)	0.3998(7)	1.3(2)
O11	0.6496(13)	0.4388(14)	0.9372(5)	0.8(2)
O12	0.8953(20)	0.4100(15)	0.7780(8)	1.7(2)
O13	0.3964(18)	0.7619(13)	0.7525(9)	1.7(2)
O14	0.8567(16)	0.8299(11)	0.3718(7)	1.2(2)
O15	0.1242(14)	0.2139(14)	0.9296(7)	1.2(2)
O16	0.2890(19)	0.5699(14)	0.4776(8)	1.3(2)
O17	0.6225(20)	0.0247(12)	0.9148(9)	2.0(2)
O18	0.4304(17)	0.8269(15)	0.2853(8)	1.7(2)
O19	0.4364(16)	0.1799(11)	0.7733(6)	0.8(2)
O20	0.6045(12)	0.4734(10)	0.6262(6)	1.5(2)
O21	0.4558(15)	0.7175(10)	0.0579(6)	1.4(2)
O22	0.7784(15)	0.9973(10)	0.2377(6)	1.4(2)
O23	0.1982(14)	0.0296(9)	0.0729(6)	1.2(2)
O24	0.9584(13)	0.7009(11)	0.0528(6)	1.5(2)
O25	0.1977(19)	0.3734(13)	0.3123(6)	2.0(2)
O26	0.4242(16)	0.3487(11)	0.0852(6)	1.4(2)

* Composition $\text{O}_{0.53} + \text{F}_{0.47}$.

Table 4. Characteristics of coordination polyhedra

Site	Composition ($Z = 1$)	Coordination number	Cation–anion distance, Å		
			minimum	maximum	mean
<i>M1</i>	0.48Nb + 0.28Mn + 0.24Ti	6	1.91(1)	2.167(8)	2.043
<i>M2</i>	0.82Ti + 0.18Mg	6	1.93(1)	2.229(9)	2.043
<i>M3</i>	0.65Ti + 0.35Nb	6	1.787(8)	2.178(8)	1.96
<i>M4</i>	0.65Ti + 0.35Fe ²⁺	6	1.81(1)	2.14(1)	1.97
Si1	1Si	4	1.621(9)	1.666(8)	1.644
Si2	1Si	4	1.588(7)	1.640(7)	1.604
Si3	1Si	4	1.551(8)	1.638(8)	1.605
Si4	1Si	4	1.599(9)	1.655(7)	1.621
P1	1P	4	1.546(8)	1.60(1)	1.56
P2	1P	4	1.49(1)	1.544(7)	1.54
Na1	1Na	6	2.300(8)	2.74(1)	2.47
Na2	1Na	6	2.19(1)	2.66(1)	2.44
Na3	0.67Na + 0.33Ca	8	2.24(1)	2.984(8)	2.52
Na4	1Na	7	2.19(1)	2.92(1)	2.51
Na5	1Na	8	2.32(1)	2.79(1)	2.57
Na6	1Na	6	2.27(1)	2.81(1)	2.46
Na7	1Na	6	2.22(1)	2.94(1)	2.49
Na8	1Na	5	2.22(1)	2.97(1)	2.43
Na9	1Na	8	2.23(1)	2.762(9)	2.55
Na10	1Na	4	2.18(1)	2.40(1)	2.30

$\text{Na}_{11}\text{TiNb}_2(\text{Si}_2\text{O}_7)_2(\text{PO}_4)_2\text{O}_3(\text{F},\text{OH})$. The main difference between β -lomonosovite and lomonosovite is that the oxygen atoms at unoccupied vertices of the PO_4 tetrahedra are replaced with OH groups. In this context, the $[\text{HPO}_4]$ and $[\text{H}_2\text{PO}_4]$ tetrahedral complexes are formed; the hydrogen bonds produced by these complexes link them into chains. The β -lomonosovite structure was repeatedly studied on samples from the Lovozero massif [10–12]. The most thorough investigations of the cation distribution over the octahedral sites in the *O* and *H* layers were carried out for a disordered modification of β -lomonosovite $[\text{Na}_{1.22}(\text{Ti}_{0.8}\text{Fe}_{0.2}^{2+})_2\text{O}_4][\text{Na}_{1.28}(\text{Ti}_{0.8}\text{Nb}_{0.2})(\text{Ti}_{0.4}\text{Nb}_{0.2}\text{Fe}_{0.25}^{3+}\text{Mn}_{0.15})][\text{Si}_2\text{O}_7]_2[\text{PO}_2(\text{OH})_2]_2(\text{Na}_{3.05}\text{Ca}_{0.5})$ [13] and β -lomonosovite from the Khibiny massif (Rasvumchorr mountain) $(\text{Na},\text{Ca},\text{K},\text{Mn},\text{Fe}^{2+})_4(\text{Ti},\text{Nb},\text{Fe}^{3+},\text{Mg})_4\text{O}_2(\text{O},\text{OH},\text{F})_2\text{Si}_2\text{O}_7]_2[\text{H}_2\text{PO}_4]_2$ [14]. The summarized data on all currently known structural and chemical varieties of β -lomonosovite and its generalized formula were given in [15].

Vuonnemite (Table 5) is topologically close to lomonosovite but differs significantly in the chemical composition (in particular, by high niobium content), Ti–Nb ordering, and the ratio of octahedrally coordinated cations and silicon. The titanium and niobium dis-

tributions over sites in the three-layer packet were determined on samples from the Ilimaussaq (Greenland) and Lovozero deposits [20] in the centrosymmetric version. For a partially hydrated vuonnemite variety from the Lovozero alkaline massif [16], the crystallochemical formula $[(\text{H}_2\text{O})_4\text{Na}_{3.7}][\text{Na}_{2.7}\text{TiMn}_{0.3}][(\text{Nb},\text{Ti})_2(\text{Si}_2\text{O}_7)_2][\text{PO}_4]_2\text{H}_4\text{O}_3\text{F}$ was derived and the detailed impurity distribution over sites of the structure identified within the sp. gr. *P1* was established (Table 5).

Lomonosovite readily loses the interpacket “filling” (Na^+ and PO_4^{3-} ions) and is hydrated, passing to murmanite $\text{Na}_4\text{Ti}_4(\text{Si}_2\text{O}_7)_2\text{O}_4 \cdot 4\text{H}_2\text{O}$. Even in the early study by N.V. Belov and N.I. Organova [21] it was established that lomonosovite is easily washed out with water under laboratory conditions not only upon heating but also at low temperatures. The main difference between murmanite and lomonosovite is that Na and P atoms in the interpacket space are replaced with water molecules; as a result, the period *c* decreases by 2.7 Å and the packet bonding weakens. The low quality of the murmanite crystal (and the corresponding experimental data) did not make it possible to reliably establish the distribution of small amounts of impurity elements over structural sites in the sp. gr. *P1* [22]. It was only found that there are 0.4 niobium atoms per formula in the *H*-layer octahedron. A more detailed

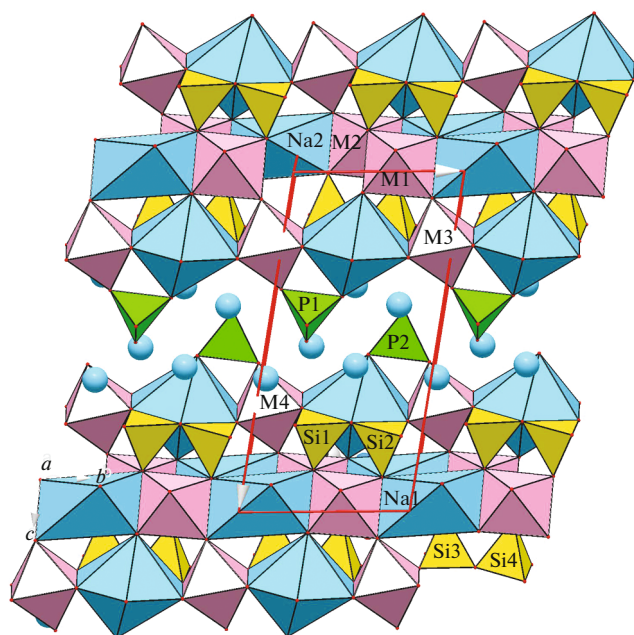


Fig. 1. Lomonosovite structure projected on the (100) plane.

impurity distribution was presented in [5, 17] within the sp. gr. $P\bar{1}$ (Table 5).

Lomonosovite is also a parent compound of the evolution series leading to the formation of some other murmanite-related minerals: calciomurmanite $(\text{Na}, \square)_2\text{Ca}(\text{Ti}, \text{Mg}, \text{Nb})_4[\text{Si}_2\text{O}_7]_2\text{O}_2(\text{OH}, \text{O})_2(\text{H}_2\text{O})_4$ [6], vigrishinite $\text{Zn}_2\text{Ti}_{4-x}\text{Si}_4\text{O}_{14}(\text{OH}, \text{H}_2\text{O})_8$ [19], and kolskyite $(\text{Ca}\square)\text{Na}_2\text{Ti}_4(\text{Si}_2\text{O}_7)_2\text{O}_4(\text{H}_2\text{O})_7$ [18]. As can be seen in Table 5, although the set of elements is almost identical, the niobium-rich lomonosovite vari-

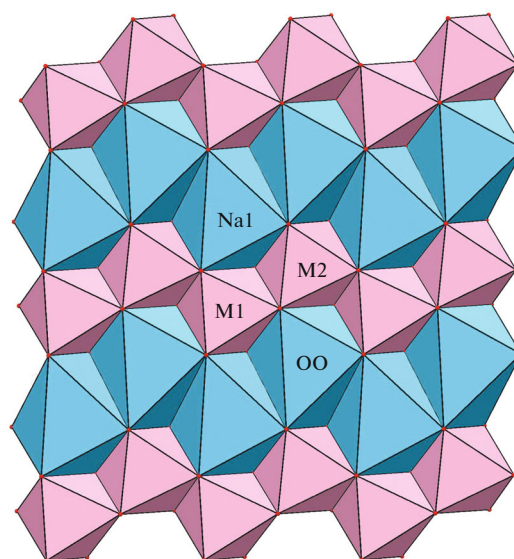


Fig. 2. O layer of octahedra in the lomonosovite structure.

ety under study differs from the previously investigated minerals [5, 17]: niobium atoms are localized in two octahedra rather than enter all four octahedra as a minor impurity. As was established in [6, 17–19], the same impurity amounts of niobium are present in transformation minerals: murmanite, calciomurmanite, vigrishinite, and kolskyite at some preferred occupation with niobium of O-layer octahedra in some cases and H-layer octahedral in other cases. Di- and trivalent cations (manganese, iron, and magnesium) are mainly localized in the O-layer octahedral or (more rarely) distributed in the O- and H-layer octahedra.

Table 5. Composition of the key sites in the structures of lomonosovite and related minerals

Mineral (sp. gr.)	M1	M2	M3	M4	References
	<i>O</i> layer			<i>H</i> layer	
Lomonosovite (<i>P1</i>)	$\text{Nb}_{0.48}\text{Mn}_{0.28}\text{Ti}_{0.24}$	$\text{Ti}_{0.82}\text{Mg}_{0.18}$	$\text{Ti}_{0.65}\text{Nb}_{0.35}$	$\text{Ti}_{0.65}\text{Fe}_{0.35}^{2+}$	This study
Lomonosovite ($P\bar{1}$)	$\text{Ti}_{1.31}\text{Nb}_{0.20}\text{Mn}_{0.22}\text{Zr}_{0.11}\text{Fe}_{0.05}^{2+}\text{Mg}_{0.05}$		$\text{Ti}_{1.52}\text{Nb}_{0.31}\text{Fe}_{0.06}^{3+}\text{Fe}_{0.05}^{2+}\text{Mn}_{0.05}\text{Ta}_{0.01}$		[5]
Lomonosovite ($P\bar{1}$)	$\text{Ti}_{0.67}\text{Mn}_{0.25}\text{Nb}_{0.08}$		$\text{Ti}_{0.93}\text{Nb}_{0.07}$		[17]
β -Lomonosovite (<i>P1</i>)	$\text{Ti}_{0.8}\text{Fe}_{0.2}^{3+}$	$\text{Ti}_{0.8}\text{Fe}_{0.2}^{3+}$	$\text{Ti}_{0.8}\text{Nb}_{0.2}$	$\text{Ti}_{0.4}\text{Nb}_{0.2}\text{Mn}_{0.15}^{2+}\text{Fe}_{0.25}$	[13]
β -Lomonosovite ($P\bar{1}$)	$(\text{Ti}_{0.83}\text{Fe}_{0.17})_2$		$(\text{Ti}_{0.987}\text{Nb}_{0.013})_2$		[14]
Vuonnemite (<i>P1</i>)	$\text{Na}_{0.7}\text{Mn}_{0.3}$	Ti	Nb	$\text{Nb}_{0.8}\text{Ti}_{0.2}$	[16]
Murmanite ($P\bar{1}$)	$\text{Ti}_{1.40}\text{Nb}_{0.29}\text{Mn}_{0.19}\text{Mg}_{0.07}\text{Fe}_{0.04}^{3+}\text{Zr}_{0.01}$		$\text{Ti}_{1.67}\text{Nb}_{0.22}\text{Fe}_{0.11}^{3+}$		[5]
Murmanite ($P\bar{1}$)	$\text{Ti}_{0.67}\text{Mn}_{0.30}\text{Nb}_{0.02}$		$\text{Ti}_{0.89}\text{Nb}_{0.11}$		[17]
Calciomurmanite ($P\bar{1}$)	$\text{Ti}_{0.42}\text{Mg}_{0.21}\text{Mn}_{0.15}\text{Nb}_{0.14}\text{Fe}_{0.08}$		$\text{Ti}_{0.94}\text{Nb}_{0.06}$		[6]
Kolskyite ($P\bar{1}$)	$\text{Ti}_{1.56}\text{Mn}_{0.23}\text{Nb}_{0.10}\text{Fe}_{0.10}^{2+}\text{Zr}_{0.01}$		$\text{Ti}_{1.37}\text{Nb}_{0.36}\text{Mg}_{0.17}\text{Mn}_{0.10}$		[18]
Vigrishinite (<i>P1</i>)	$\text{Ti}_{0.56}\text{Mn}_{0.30}\text{Nb}_{0.14}$	$\text{Ti}_{0.63}\text{Mn}_{0.30}\text{Nb}_{0.07}$	$\text{Ti}_{0.79}\text{Nb}_{0.21}$	$\text{Ti}_{0.85}\text{Nb}_{0.15}$	[19]

In all minerals presented in Table 5 (as well as in Ag-substituted lomonosovite [17] and Zn-substituted murmanite [19]), Ti dominates at octahedral *M* sites in both *O* and *H* layers, while Nb (along with other impurities) is the reason for the nonequivalence of titanium octahedra, although the central symmetry of the structure is retained in some minerals. An exception is vuonnemite, in which niobium dominates in both octahedra of the *H* layer, while Ti is replaced with sodium in one octahedron of the *O* layer.

It is noteworthy that the octahedra in the same layer are equally filled in cation-substituted forms of lomonosovite and murmanite (sp. gr. $P\bar{1}$), whereas in vigrishinite their degrees of filling differ significantly (sp. gr. *P1*). One can suggest that vigrishinite inherits this ordering from parent lomonosovite. If this suggestion is true, one can conclude that ordered lomonosovite is not an endemic mineral of the Khibiny massif but existed also in the Lovozero massif.

CONCLUSIONS

A new structural and chemical lomonosovite variety was found and studied. It differs from the “normal” lomonosovite by not only a high niobium content (about one atom per unit cell), but also (which is especially important) presence of a structural site where Nb is a dominant cation. This circumstance somehow relates this lomonosovite variety and vuonnemite. However, the distribution of highly charged cations over sites differs from that in vuonnemite, where niobium occupies both nonequivalent octahedra of the *H* layer and barely enters octahedra of the *O* layer [15, 16] (whereas in the structure of niobium-rich lomonosovite it enters octahedra of both layers). Significant differences between lomonosovite and vuonnemite are also observed in the topology and composition of the octahedral *O* layer, filled in ratios of 1 Na : 1 Ti (for ideal lomonosovite) and 3 Na : 1 Ti (for ideal vuonnemite). The lomonosovite variety yields additional data on the concentration of rare elements in titanosilicate minerals.

ACKNOWLEDGMENTS

We are grateful to V.G. Senin for performing the microprobe analysis. This study was performed at the Shared Equipment Center of the Federal Scientific Research Centre “Crystallography and Photonics,” Russian Academy of Sciences.

FUNDING

This study was supported by the Ministry of Science and Higher Education of the Russian Federation (project no. RFMEFI62119X0035) within a State assignment for the Federal Scientific Research Centre “Crystallography and Photonics” (Russian Academy of Sciences) in the part con-

cerning the X-ray diffraction analysis and within a State assignment for the Vernadsky Institute of Geochemistry and Analytical Chemistry of the Russian Academy of Sciences in the part concerning the chemical investigation of the material and by the Russian Foundation for Basic Research, project no. 18-29-12005, in the part concerning the crystallochemical analysis of lomonosovite-group layered minerals.

REFERENCES

1. V. I. Gerasimovskii, Dokl. Akad. Nauk SSSR **70** (1), 83 (1950).
2. A. D. Khalilov, E. S. Makarov, K. S. Mamedov, and L. Ya. P'yanzina, Dokl. Akad. Nauk SSSR **162**, 179 (1965).
3. R. K. Rastsvetaeva, V. I. Simonov, and N. V. Belov, Dokl. Akad. Nauk SSSR **197** (1), 81 (1971).
4. N. V. Belov, G. S. Gavrilova, L. P. Solov'eva, and A. D. Khalilov, Dokl. Akad. Nauk SSSR **235**, 1064 (1977).
5. F. Camara, E. Sokolova, F. C. Hawthorne, and Y. Abdu, Mineral. Mag. **72** (6), 1207 (2008).
6. I. S. Lykova, I. V. Pekov, N. V. Chukanov, et al., Eur. J. Mineral. **28** (4), 835 (2016).
7. V. I. Andrianov, Kristallografiya **32** (1), 228 (1987).
8. R. K. Rastsvetaeva and S. M. Aksenov, Crystallogr. Rep. **56** (6), 910 (2011).
9. G. Ferraris and A. Gula, Mineral. Geochem. **57**, 69 (2005).
10. R. K. Rastsvetaeva, M. I. Sirota, and N. V. Belov, Kristallografiya **20** (2), 259 (1975).
11. R. K. Rastsvetaeva, Kristallografiya **31** (6), 1070 (1986).
12. R. K. Rastsvetaeva, Kristallografiya **34** (4), 880 (1989).
13. R. K. Rastsvetaeva, Zap. Vses. Mineral. O-va, No. 6, 696 (1988).
14. O. V. Yakubovich, O. V. Karimova, O. A. Ageeva, and B. E. Borutskii, Zap. Vseross. Mineral. O-va, No. 6, 88 (2014).
15. I. S. Lykova, N. V. Chukanov, I. V. Pekov, et al., Eur. J. Miner. **30** (2), 289 (2018).
16. R. K. Rastsvetaeva, S. M. Aksenov, I. A. Verin, and I. S. Lykova, Crystallogr. Rep. **56** (3), 407 (2011).
17. I. S. Lykova, I. V. Pekov, N. V. Zubkova, et al., Eur. J. Mineral. **27** (4), 535 (2015).
18. F. Camara, E. Sokolova, Y. Abdu, et al., Can. Mineral. **51**, 921 (2013).
19. I. S. Lykova, I. V. Pekov, N. V. Zubkova, et al., Eur. J. Mineral. **27** (5), 669 (2015).
20. T. S. Ercit, M. A. Cooper, and F. C. Hawthorne, Can. Mineral. **36**, 1311 (1998).
21. N. V. Belov and N. I. Organova, Geokhimiya, No. 1, 4 (1962).
22. R. K. Rastsvetaeva and V. I. Andrianov, Kristallografiya **31** (1), 82 (1986).

Translated by Yu. Sin'kov